Environmental Science & Technology

pubs.acs.org/est

Article

Micro- and Nanoplastics in Alpine Snow: A New Method for Chemical Identification and (Semi)Quantification in the Nanogram Range

Dušan Materić,* Anne Kasper-Giebl, Daniela Kau, Marnick Anten, Marion Greilinger, Elke Ludewig, Erik van Sebille, Thomas Röckmann, and Rupert Holzinger

Cite This: *Environ. Sci. Technol.* 2020, 54, 2353−2359

Read Online

ACCESS | Metrics & More | Article Recommendations | Supporting Information

ABSTRACT: We present a new method for chemical characterization of micro- and nanoplastics based on thermal desorption−proton transfer reaction−mass spectrometry. The detection limit for polystyrene (PS) obtained is <1 ng of the compound present in a sample, which results in 100 times better sensitivity than those of previously reported by other methods. This allows us to use small volumes of samples (1 mL) and to carry out experiments without a preconcentration step. Unique features in the high-resolution mass spectrum of different plastic polymers make this approach suitable for fingerprinting, even when the samples contain mixtures of other organic compounds. Accordingly, we got a positive fingerprint of PS when just 10 ng of the polymer was present within the dissolved organic matter of snow. Multiple types of microplastics (polyethylene terephthalate (PET), polyvinyl chloride, and polypropylene carbonate), were identified in a snowpit from the Austrian Alps; however, only PET was detected in the nanometer range for both snowpit and surface snow samples. This is in accordance with other publications showing that the dominant form of airborne microplastics is PET fibers. The presence of nanoplastics in high-altitude snow indicates airborne transport of plastic pollution with environmental and health consequences yet to be understood.

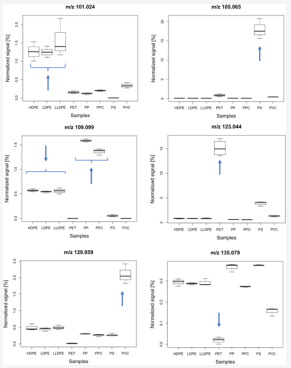

INTRODUCTION

Micro- and nanoplastics are well recognized as environmental pollutants. They are present in most environmental habitats and can potentially affect organisms in ways that are not completely understood.[1] Much of the scientific research studies on plastic polymers in the environment has focused on microplastics in the marine environment (particles, <5 mm),[2,3] and only recently, nanoplastics (<1 μm) have been successfully analyzed.[4]

Various methods are used in microplastic research; however, when a polymer fragment gets to the nanoscale, conventionally used optical and chemical methods are not suitable anymore (sensitivity issues and physical and optical limits). The lack of suitable analytical tools results in a perceived knowledge gap in our understanding of the nanoplastics.[5,6]

Here, we present a highly sensitive method for detection, speciation, and quantification of micro- and nanoplastics based on thermal desorption−proton transfer reaction−mass spectrometry (TD-PTR-MS). The detection technique, PTR-MS, is widely used in the analysis of various complex organic mixtures in the environment including real-time monitoring of volatile organic compounds, semivolatiles, and organic aerosols in air and, recently, dissolved organic matter (DOM) in environmental waters and ice.[7−11]

A particular strength of the TD-PTR-MS method is the combination of high sensitivity and high-mass resolution.[9,10] While the latter allows chemical identification of the compounds to the level of chemical formula, high sensitivity provides quantitative information of the low-concentrated organics. In addition, required sample sizes are small, which makes this method suitable for high-throughput analysis.

In this work, for the first time, we applied the TD-PTR-MS method to the analysis of common micro- and nanoplastics polymers. We developed a fingerprint algorithm for polymer identification when present in a complex organic matrix, such as dissolved organic matter in snow, and successfully identified micro- and nanoplastic polymers in snow samples collected in the Alps at 3 km above sea level.

MATERIALS AND METHODS

Standards' Preparation. A small amount of different plastic polymers was grinded with a fine metal saw, and pieces of <0.3 mm were used for further analysis. We used polyethylene terephthalate (PET), high-density polyethylene (HDPE), low-density polyethylene (LDPE), linear low-density polyethylene (LLDPE), polypropylene (PP), polypropylene carbonate (PPC), polyvinyl chloride (PVC), and polystyrene (PS). The polymers were provided by the TCR Plastics,

Received: December 11, 2019
Revised: January 8, 2020
Accepted: January 17, 2020
Published: January 17, 2020

Netherlands, except PET, PP, and PS, which were taken from the clean end products (plastic bottle, laboratory tubes, and laboratory cold storage material, respectively). One grain of the polymer was loaded into clean 10 mL vials, and for each type, we prepared triplicate samples and used empty vials as procedural blanks.

For the sensitivity test, we used PS standard spheres of 1 μm in diameter (PS-ST-1.0, Microparticles GmbH, Berlin, Germany), prepared series of solutions in water, and loaded the experimental vials to contain 1, 5, 10, 20, and 50 ng of PS. The number concentration of the PS solution was 1819 particles per 1 ng. For this experiment, we used 10 mL glass vials with a 5 mm quartz filter to provide a surface for PS particles to attach, all prebaked at 250 °C overnight.

Snow Sample Preparation. The samples were collected from the glaciers next to the Sonnblick Observatory, Austria, at about 3100 m altitude, distant to any anthropogenic activity and within the Austrian National Park Hohe Tauern. A complete snow profile was collected on April 2017, representing the complete snow accumulation for the previous winter season starting in October, reaching an absolute depth of 3.9 m. Sampling was performed in 20 cm sections, which were taken with a stainless steel cylinder. For this project, we have analyzed three samples at nominal section depths of 2.6, 2.8, and 3.0 m, as this part of the profile was preserved as compact cores with 5.6 cm diameter, suitable for excluding possible contamination at the surfaces that can occur during sampling or storage. The outer 1 cm of the surface was shaved off with a clean ceramic knife, a longitudinal subsample was taken for the measurement (not filtered), and the rest of the core was gently melted in a microwave and mixed with a clean glass stick. The longitudinal subsamples were melted at room temperature resulting in 20−30 mL of each sample. The samples were well hand-mixed (homogenized), but not vortexed, to avoid possible fragmentation of microplastics. From the rest of the melted core (approximately 0.5 L), 10 mL was subsampled and filtered through a 0.2 μm pore size PTFE filter to separate microplastics from nanoplastics. Process blanks were prepared by exposing a similar amount of Milli-Q water to the same containers and surfaces for the same amount of time including the laboratory materials such as syringes, pipette tips, and filters.

Surface snow samples were taken in the periods 2017-03-20 to 2017-04-01 close to the Sonnblick Observatory, and analyses were performed as previously described.[10] Mass spectra of the surface snow samples were already analyzed and interpreted with respect to organic aerosol deposition dynamics.[12] For the work presented here the original mass spectra were re-evaluated addressing the presence of nanoplastics.

TD-PTR-MS. Low-pressure evaporation/sublimation was performed as described in our previous work.[9] We used the TD-PTR-MS protocol and parameters as stated earlier (ramping from 35 to 350 °C at 40 degrees/min, E/N 120 Td).[10,11] For the data processing, we used the custom-made software package PTRwid.[13] The PTR-MS signal was integrated over 10 min starting when the TD temperature reached 50 °C. This way, the thermal degradation of each polymer (which produces different degradation products at different temperatures) was integrated in the analysis. No compound has been observed in carry-over tests, suggesting that thermal desorption was complete regardless of the type and size of the polymers present. The thermograms of all the plastic types and all the ions are included in the Supporting Information.

The mass spectra of each measurement were corrected for a blank signal, and masses below the 3σ detection limit were not considered for analysis. For PCA and fingerprinting analysis, we only used ions with m/z > 100.

Fingerprinting Algorithms. We developed four fingerprinting algorithms to score the similarity between mass spectra of a standard material (further referred as library mass spectra) and a sample. The algorithms 1 and 2 (ALG1 and ALG2) select the highest n ion signals (e.g., 20) above m/z 100 and normalize the signal to the highest peak. The algorithms 3 and 4 (ALG3 and ALG4) normalize the signal to the sum of all peaks.

ALG2 and ALG4 calculate the absolute difference (msDIFF) from the library mass spectra as

$$\text{msDIFF} = \sum_{i=1}^{n} |\text{mz}_{\text{Si}} - \text{mz}_{\text{Li}}| \quad (1)$$

where mz_s is the normalized concentration of the sample for ion i and mz_L is the normalized concentration in the library mass spectrum for ion i. The ratio of msDIFF in eq 1 to the maximal theoretical difference (i.e., when the library and the sample mass spectrum share no common ion) returns a value between 0 and 1 (i.e., 0 is identical and 1 is 100% different, see the script in the Supporting Information for more details).

In ALG1 and ALG3, the difference for each ion is weighted by the normalized ion intensity (eq 2) and normalized to the maximal possible difference, again resulting in a value between 0 and 1.

$$\text{msDIFF} = \sum_{i=1}^{n} (|\text{mz}_{\text{Si}} - \text{mz}_{\text{Li}}| \times \text{mz}_{\text{Li}}) \quad (2)$$

where mz_s is the normalized concentration of the sample for ion i and mz_L is the normalized concentration in the library mass spectrum for ion i. This way, in ALG2 and ALG4, the library ions with higher concentrations are proportionally valued higher in the calculation of the total difference. For example, an absolute difference (msDIFF_i) of 1 for the library ion with the relative concentration 100% (the highest ion) would be weighted with a factor 1; however, the weighting factor for the library ion with the relative concentration 50% would be 0.5.

Following calculating the total differences (msDIFF), the algorithms calculate the mass spectra similarity (match score) as

$$M = 1 - \text{msDIFF} \quad (3)$$

The fingerprinting evaluation (e.g., false positive and false negative) can be found in the Supporting Information Figure S1 and Table S1.

Fingerprinting the Samples. We performed the fingerprinting for all the samples and all the blanks (available in the Supporting Information) using a script developed for this purpose (also available in the Supporting Information). Considering all the challenges associated with the complex organic matrix in snow (Table S1), for the fingerprinting, we used the 30 most abundant library ions with m/z > 100. Smaller-molecular-weight ions were excluded in the fingerprinting as they may contain higher levels of ions coming from the organic matrix and not the polymers.

https://dx.doi.org/10.1021/acs.est.9b07540
Environ. Sci. Technol. 2020, 54, 2353−2359

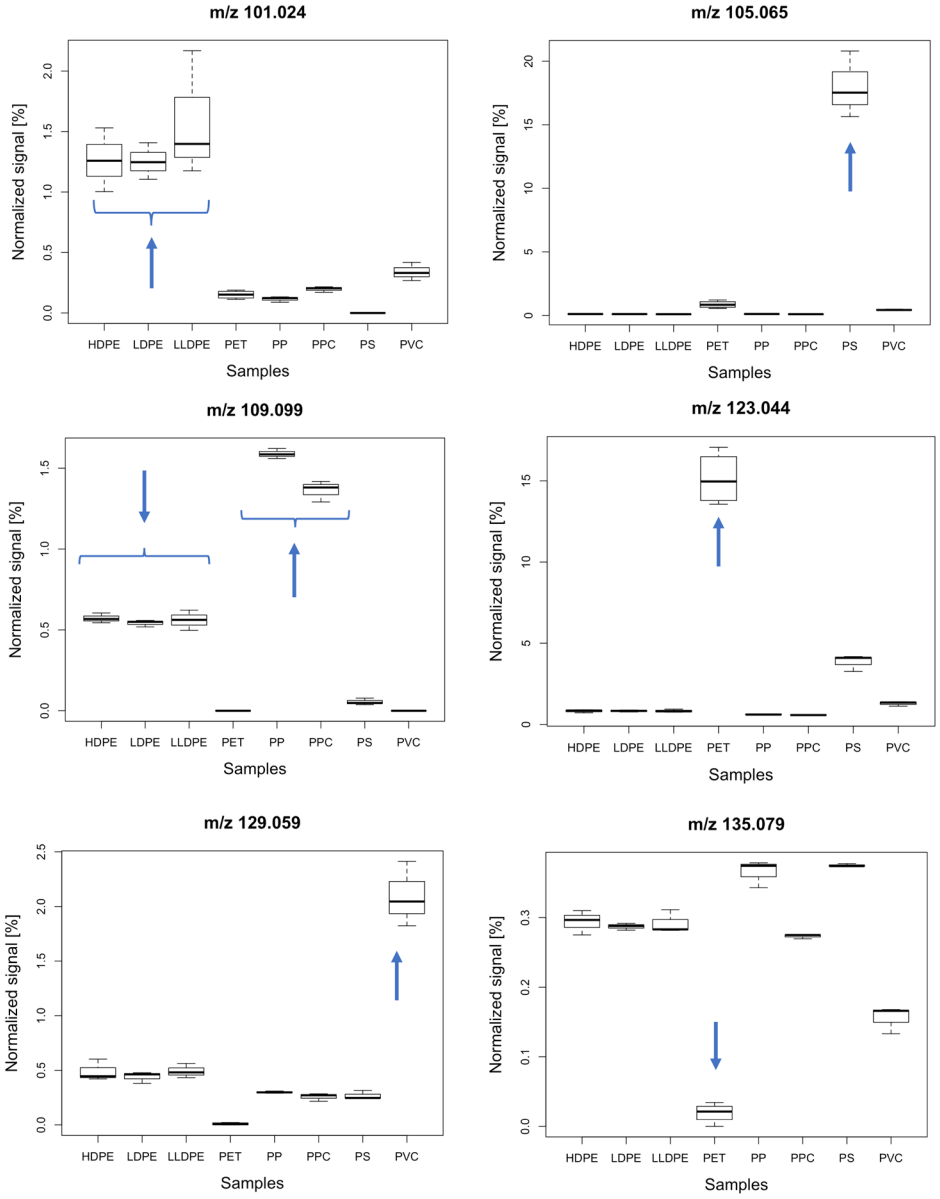

Figure 1. Example of ions obtained by the analysis of the pure polymer, which can be used to identify and distinguish the different types of plastics. HDPE, high-density polyethylene; LDPE, low-density polyethylene; LLDPE, linear low-density polyethylene; PET, polyethylene terephthalate; PP, polypropylene; PPC, polypropylene carbonate; PS, polystyrene; and PVC, polyvinyl chloride. The signal is normalized to the total concentration of all the ions. The arrows are added to highlight the differences between plastic types.

The principle of the quantification protocol for PTR-MS and TD-PTR-MS was explained earlier.[9,11,14−16] In short, due to the extensive knowledge of physics behind proton transfer reaction in the instrument reaction chamber (drift tube), the compound concentrations $[C]$ can be calculated from ion signals as follows:

$$[C] = \frac{1}{kt} \times \frac{[\mathrm{M{\cdot}H^+}]}{[\mathrm{H_3O^+}]} \times \frac{\sqrt{(m/z)_{\mathrm{H_3O^+}}}}{\sqrt{(m/z)_{\mathrm{M{\cdot}H^+}}}} \quad (4)$$

where k is the reaction rate coefficient, t is the residence time of the primary ions in the drift tube, $[\mathrm{M{\cdot}H^+}]$ and $[\mathrm{H_3O^+}]$ are the ion counts representing the protonated analyte and primary ions, respectively, and $(m/z)_{\mathrm{H_3O^+}}$ and $(m/z)_{\mathrm{M \cdot H^+}}$ represent the mass-of-charge of protonated water and the analyte M, respectively.

Quantification of the polymers in this work was based on the 30 ions that matched the library mass spectra. The quantification calculation from eq 4 was improved in this work via preservation of the ratio of the ion signal from the plastics library so that possible contamination from natural DOM was excluded. For example, if compounds from natural DOM produce one or more ions with the exact mass as the nanoplastic polymer, to prevent overestimation, such ion signals are reduced according to the expected values calculated from the library ions of that particular polymer (for more, see the scripts in the Supporting Information).

Using the 30 ions from the library and the known concentration of PS, we obtained a recovery of 15% (Figure S2), corresponding to an underestimation factor of 6.7 for polystyrene. This recovery level is between previously reported values for DOM (12%) and tests with semivolatile standards (e.g., levoglucosan and glutaric acid, 62% and 18%,

https://dx.doi.org/10.1021/acs.est.9b07540
Environ. Sci. Technol. 2020, 54, 2353−2359

respectively).[11,17] This is likely due to thermal degradation and PTR efficiency resulting in not detectable fragments/molecules (neutral fragments, CO, CO_2, etc.). Future improvement in instrument coating, ionization optimization, and utilizing different carrier gasses may improve the recovery rate. However, this does not affect the quantification as (1) ion yields are stable and (2) an appropriate correction factor can be used, (e.g., for PS). The correction factors and recovery rates for polymers other than PS are expected to be of a similar magnitude (i.e., between DOM and other semivolatiles); however, no nanoplastic standards are yet available to test this.

In this work, the correction factors are not applied. Thus, the reported concentrations of the polymers found in the snow/ice samples reported here are semiquantitative values, not corrected for TD/PTR recovery and losses during sample treatment (e.g., filtration), and as such they represent low thresholds for the concentrations.

Quality Control. Contamination with microplastics and nanoplastics from the sampling equipment and laboratory materials or during the preparation for the analysis can pose a severe threat to the quality of the results, so adequate procedures should be adopted depending on the nature of the experiment.

For our snowpit samples, to exclude possible contamination from the equipment during the sampling, we shaved the outside (~1 cm) of the sample cores before sampling for our analysis. To assess possible contamination during sample storing and measurement, we performed procedural blank tests in which we exposed Milli-Q water to all laboratory materials we used.

For the surface snow samples, field blanks were taken at the sampling site by exposing Milli-Q water to the impurities of the equipment in the sampling process in order to quantify possible sampling contamination. These blanks were also processed in the same way as the samples to evaluate other sources of contamination during the analysis.

Although samples and blanks were stored in HDPE bags (snow core samples) or PP containers (surface snow samples), no PE or PP fingerprint has been found in any of samples or blanks. Moreover, no positive fingerprint of any type of plastics was found in the blanks (see the Supporting Information), which excludes significant contamination during sampling, storage, and analysis.

RESULTS AND DISCUSSION

Thermal desorption followed by PTR-MS analysis of plastic polymers results in rich mass spectra containing more than 300 ions of different masses. Different polymers of plastics express various unique features (pointed by arrows), which can be used for the identification (Figure 1). For example, the ion m/z 105.065 (Figure 1, top right), corresponding to $C_8H_9^+$ (protonated styrene), is a thermal decomposition product of polystyrene that can be used for its quantification, with a little or no interference by the ions from the other polymers. The polyethylene varieties (HDPE, LDPE, and LLDPE) show clearly elevated levels at m/z 101.024 ($C_4H_4O_3H^+$), PET at m/z 123.044 ($C_7H_6O_2H^+$), and PVC at m/z 129.059 ($C_6H_8O_3H^+$).

Using calibration standards, the unique ions present in the mass spectrum of a certain polymer can be used for micro- and nanoplastic quantification. In a calibration experiment with polystyrene, we obtained a sensitivity of 23 ppt gas-phase concentration of an ion with m/z 105.069 per ng solid sample material (over the 10 min TD time) (see Figure 2). The calculated detection limit (3σ of the blanks) for ion m/z

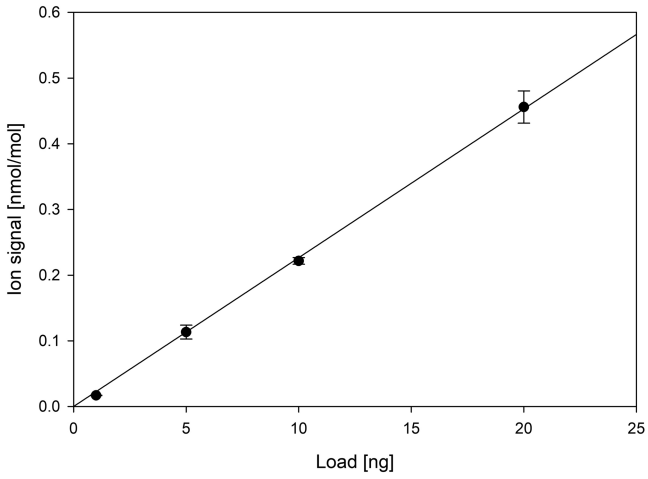

Figure 2. Sensitivity and linearity test of polystyrene ion m/z 105.069. Error bars represent standard deviation (n = 4; R^2 = 0.9998). The linear fit is forced through the origin.

105.069 is 7.8 ppt (0.34 ng); thus, we can successfully quantify subnanogram concentrations of pure polystyrene in a sample. This sensitivity is ~100 times higher than that of previously reported methods[5,6,18] and allows the analysis of various environmental samples (e.g., samples of snow, rain, and drinking water) without a preconcentration step, with sample volumes as low as 1 mL. From Figure 1, we can also notice that some polymers have an insignificantly different expression of single-ion signals (e.g., HDPE, LDPE, and LLDPE). In the case of ion m/z 109.099 ($C_8H_{13}^+$) of PP and PPC (Figure 1), the single-ion approach does not allow analytical separation.

The single-ion identification presented in Figure 1 is illustrative but does not fully exploit the richness of the mass spectra. In addition, identification with single ions is likely challenging when the plastic polymers are present in a mixture with other organics (e.g., DOM). Figure 3 shows that most types of plastics can be clearly distinguished by principal component analysis (PCA), which is a multivariate approach where more ions are considered to improve the separation. PCA of the PTR-MS data for all the polymers used in this work illustrates clustering for all types of plastics except PE of different densities (LDPE, LLDPE, and HDPE) and PP/PPC. In the following, we exploit these differences in our sensitive method for plastic fingerprinting when different types of plastics are present within a natural organic matrix (see the Materials and Methods section and Supporting Information).

It is challenging to successfully fingerprint the plastic polymers when they are present together with other organics. In complex organic mixtures, such as DOM in snow, ions of the same m/z as those from the plastic polymers can also be present in significant abundance, which could mask the typical micro/nanoplastic signal. On the other hand, the strict detection limit applied in the data processing could result in detection of only highly abundant polymer ions; whereas, low-abundant ions close to the detection limit get filtered out. A suitable method, algorithm, and analysis strategy should successfully deal with these challenges reducing the possibility of both false-positive and false-negative results. In the Supporting Information, we showed that the selection of the

https://dx.doi.org/10.1021/acs.est.9b07540
Environ. Sci. Technol. 2020, 54, 2353−2359

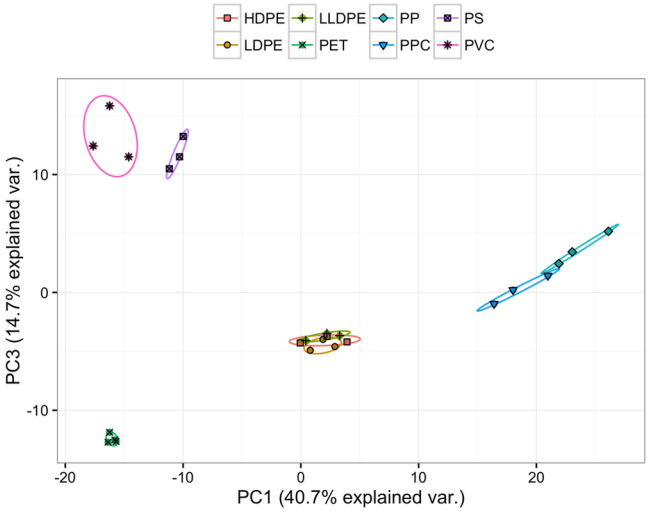

Figure 3. PCA of different plastic polymers considering ions of >100 m/z. HDPE, high-density polyethylene; LDPE, low-density polyethylene; LLDPE, linear low-density polyethylene; PET, polyethylene terephthalate; PP, polypropylene; PPC, polypropylene carbonate; PS, polystyrene; and PVC, polyvinyl chloride.

30 most concentrated ions with m/z > 100 allows successful fingerprinting within the complex organic mixture of snow samples when a cutoff score of >60% is used. Other algorithms facilitating a more "guided" approach (e.g., considering just a preselected list of ions) could be valuable for the fingerprinting, especially after the removal of the organic matrix, but they are not addressed in this pilot study.

As the first scientific application, we used the new technique for detection and quantification of different types of plastic polymers in high-altitude surface snow and snowpit samples. Re-analysis of the surface snow PTR-MS mass spectra obtained in our previous work[10] revealed positive fingerprints for PET for all the samples except the sample collected on 2017-03-26, which had a match score of 57%, thus just below the set threshold (60%). Successful fingerprinting (the level of the match score) depends on the concentration of the polymers in the sample. For instance, although the match score was below the threshold for the sample 2017-03-26, we calculated the concentration of PET to be 27 ng/mL (Table 1), which is elevated compared to those of the previous and later sampling periods (~40% higher). The lower match score may be due to the presence of other organics from the matrix with the same m/z as the PET ion products, decreasing the match score below the threshold. Thus, there is a trade-off between a good match score and potential overestimation in the quantification. In other words, if the presence of the other organic ions masking the polymer signal is substantially high, this can result in a negative match to prevent a severe overestimation of the concentration by the method. Therefore, in the case of the presence of such complex organic mixtures in the sample (e.g., high DOM loads), it is advisable to remove the matrix before the analysis of the nanoplastics.

We further investigated what would be the required minimum concentration of a polymer in a complex organic matrix of snow for a positive fingerprint. Using the polystyrene as an example and the in silico addition of its mass spectrum to the mass spectra of natural samples analyzed here (75 to 661 ng/mL of DOM retrieved by PTR-MS), we obtained positive fingerprints when ~10 ng of PS was present in samples. This value could be different for different polymers and types of organic matrixes present thus should be evaluated for each experiment. We expect that this value would be much lower if a polymer preconcentration or digestion of the organic matrix is used and higher if more organics are present in the sample (e.g., high concentration of natural DOM in the samples).

The snowpit taken on April 2017 from a nearby glacier field has been sampled and, in this work, we analyzed cores of the pit section 13−15 (2.6−3.0 m in depth) because this was the best-preserved section, suitable for analysis of inner parts of the core. No precise dating was performed, but most likely, this part of the pit reflects snow samples accumulated during early winter. Chemical analysis of the melted cores showed the presence of PET, PPC, and PVC; however, after the 0.2 μm filtration only PET nanoplastics were found (Table 1).

For both the melted and filtered snow from the snowpit samples and for the surface snow, PET shows the highest concentrations among the different types of plastics, even in the fresh precipitation. In the fresh snow sample of 20th of March 2017, the fingerprint score for PET nanoplastics was 81.4 (Table 1), indicating high contribution of this polymer relative to other DOM in the fresh precipitation. These nanoparticles are most likely a product of microplastic

Table 1. Concentrations of the Different Types of Micro/Nanoplastics Observed in the Surface Snow and Snowpit Samples[a]

	melted snow			filtered snow (0.2 μm)		
sample	match	score	quantity [ng/mL]	match	score	quantity [ng/mL]
snowpit 2017, depth of 2.6 m	PET	61.5	7.0			
	PPC	64.4	16.5			
snowpit 2017, depth of 2.8 m	PET	65.8 ± 3.1	22.9 ± 13.9	PET	65.6 ± 7.7	18.5 ± 1.5
snowpit 2017, depth of 3.0 m	PET	78.2 ± 14.2	5.6 ± 0.9			
	PPC	60.9 ± 2.4	10.8 ± 4.1			
	PVC	62.6 ± 5.4	6.9 ± 0.2			
surface snow 2017-03-20	n/a		n/a	PET	81.4 ± 7.1	4.6 ± 0.9
surface snow 2017-03-23	n/a		n/a	PET	60.4 ± 9.7	18.5 ± 2.2
surface snow 2017-03-26	n/a		n/a	PET?	57.1 ± 1.5	23.6 ± 3.0
surface snow 2017-03-29	n/a		n/a	PET	70.0 ± 1.7	12.1 ± 2.3
surface snow 2017-04-01	n/a		n/a	PET	62.7 ± 2.5	13.8 ± 2.3

[a]Not corrected with an underestimation factor of ~6.7 (see Materials and Methods). Errors represent standard deviation over the triplicate of all filtered samples and duplicates for melted snow samples, except the pit sample 2.6 M (single run). All the match scores can be found in the Supporting Information.

https://dx.doi.org/10.1021/acs.est.9b07540
Environ. Sci. Technol. 2020, 54, 2353−2359

degradation of PET, which is one of the most common plastics used mostly for synthetic fibers in the clothes industry and plastic bottles for beverages. Our finding of the predominant presence of PET compared to the other polymers is consistent with previous work on urban air microplastic pollution research, where it was discovered that urban microplastics consist mostly of fibers.[19,20]

Recently, the presence of microplastics in remote areas of the Pyrenees has been reported, with higher abundance of sheets and fragments compared to fibers.[21] The chemical compounds were identified as PS and PE by a spectroscopy technique. It has also been reported that nonfiber polymer deposition correlated with the amount of precipitation during the sampling period.[19] The disagreement between the results obtained in the urban areas[19,20] (comparable with our findings in the high-altitude Alps) and the remote Pyrenees[21] raises the question of the sampling strategy that needs to be developed for atmospheric measurements of micro- and nanoplastics. Simple deposition funnels with a bottle at the bottom to collect dry and wet deposition might be inadequate and selective to heavier particles such as sheets and fragments while light fibers might escape the funnel, especially during nonprecipitation periods. However, the lack of PS in our samples might be due to the chemical changes that PS nanoparticles underwent via weathering and UV oxidation, as described previously.[22] This would result in a shift in mass spectra and change in the fingerprint, thus more research is needed to address this issue.

Concentrations of the micro/nanoplastics observed in the surface snow and snowpit samples are shown in Table 1. These concentrations were not corrected with an underestimation factor of 6.7 measured for polystyrene (see Materials and Methods) and thus represent lower limits for the actual concentrations. The filtered snowpit samples had a positive fingerprint of PET only for the sample core of 2.8 m in depth. The PET loads of unfiltered samples for the other two cores were as low as 8.9 and 8.3 ng/mL. The low abundance may explain why these compounds could not be detected with a positive fingerprint after the filtration. The minimal presence of nanoplastics in the snowpit samples compared to the surface snow samples can be likely attributed to the nanoplastic deposition processes. The surface samples show that in the fresh surface snow sample (2017-03-20), the concentration of nanoplastics was low and it increased due to dry deposition in the later precipitation-free period (Table 1). Apparently, the big precipitation events, which provide most of the snow to the pit, contain only small loads of nanoplastics. During precipitation-free periods, higher levels of nanoplastics are delivered to the snow surface by dry deposition. This potentially results in thin plastic-rich layers within the pit, which were diluted in our samples, which integrate a plastic content of 20 cm of the snow core. On the other hand, higher depositions of most of the inorganic and organic compounds are reported at the same site during spring compared to the winter snow, which might also be similar for the nanoplastics.[23−25] We suggest that higher-resolution sampling (e.g., 1 cm sections) should be used for measurements of plastics in snow and ice cores.

Total organic loads in the snow surface samples coming from different semivolatile organic compounds have been previously published (ranging from 75 to 661 ng/mL for the period).[10] Our new evaluation shows that concentrations of PET (between 5.4 and 27.4 ng/mL) for the same surface snow samples may account for several percent (3−6% in this example) of the total organics retrieved by the same method. These numbers may be affected by the instrument recovery rate. However, since TD-PTR-MS is most sensitive to the semivolatile DOM and the recovery rate 12% of the total DOM[11] is similar to the 15% found here for PS (Figure 2), our first results indicate potentially concerning levels of global atmospheric nanoplastic pollutions that are transported even to remote alpine regions. More research studies are needed to address this issue.

It is clear that the novel field of nanoplastic research in environmental samples has its challenges, especially when the polymers are present at low concentrations such as in air, snow, and natural and drinking water. The sensitivity of the TD-PTR-MS method presented here offers a novel contribution to the field, closing the methodological gap of chemical characterization and quantification at a nanogram scale. However, many unknowns still exist as a consequence of non-existent nanoplastic standards of different types and sizes. The loss during filtration, nanoplastic weathering effect, oxidation changes, and degradation protocols therefore still need to be systematically described. Further development is also needed to combine the accuracy of this sensitive chemical characterization technique with a technique that would add the size and shape information of the particles, allowing more detailed assessment of the potential harm of nanoplastics in the environment.

■ ASSOCIATED CONTENT

Supporting Information

The Supporting Information is available free of charge at https://pubs.acs.org/doi/10.1021/acs.est.9b07540.

Supplementary information containing more details on the method and associated supplementary figures and tables (PDF)

Mass spectra of PS standard different concentrations, mass spectra library of all the plastics types, snow core mass spectra, and match scores of the blanks and all the samples against all the polymer types (XLSX)

Thermograms for each plastic type and all the ions analyzed (ZIP)

Scripts and library mass spectra that were used for fingerprinting and the fingerprint method evaluation (ZIP)

■ AUTHOR INFORMATION

Corresponding Author

Dušan Materić − *Institute for Marine and Atmospheric Research, Faculty of Science, Utrecht University, 3584 CC Utrecht, The Netherlands;* orcid.org/0000-0002-6454-3456; Email: dusan.materic@gmail.com

Authors

Anne Kasper-Giebl − *Institute of Chemical Technologies and Analytics, Vienna University of Technology, Wien 1060, Austria*

Daniela Kau − *Institute of Chemical Technologies and Analytics, Vienna University of Technology, Wien 1060, Austria*

Marnick Anten − *Institute for Marine and Atmospheric Research, Faculty of Science, Utrecht University, 3584 CC Utrecht, The Netherlands*

Marion Greilinger − *Institute of Chemical Technologies and Analytics, Vienna University of Technology, Wien 1060,*

https://dx.doi.org/10.1021/acs.est.9b07540
Environ. Sci. Technol. 2020, 54, 2353−2359

Austria

Elke Ludewig − *Zentralanstalt für Meteorologie und Geodynamik (ZAMG), Vienna 1190, Austria*

Erik van Sebille − *Institute for Marine and Atmospheric Research, Faculty of Science, Utrecht University, 3584 CC Utrecht, The Netherlands*

Thomas Röckmann − *Institute for Marine and Atmospheric Research, Faculty of Science, Utrecht University, 3584 CC Utrecht, The Netherlands*

Rupert Holzinger − *Institute for Marine and Atmospheric Research, Faculty of Science, Utrecht University, 3584 CC Utrecht, The Netherlands*

Complete contact information is available at: https://pubs.acs.org/10.1021/acs.est.9b07540

Notes

The authors declare no competing financial interest.

■ ACKNOWLEDGMENTS

D.M. acknowledges the support of The Netherlands Earth System Science Centre (NESSC) research network. E.v.S. was supported through funding from the European Research Council (ERC) under the European Union's Horizon 2020 Research and Innovation Programme (grant agreement no. 715386). Snowpit sampling was performed within the ongoing monitoring program supported by the BMNT.

■ REFERENCES

(1) Bond, T.; Ferrandiz-Mas, V.; Felipe-Sotelo, M.; van Sebille, E. The Occurrence and Degradation of Aquatic Plastic Litter Based on Polymer Physicochemical Properties: A Review. *Crit. Rev. Environ. Sci. Technol.* **2018**, *48*, 685−722.

(2) Ivleva, N. P.; Wiesheu, A. C.; Niessner, R. Microplastic in Aquatic Ecosystems. *Angew. Chem., Int. Ed.* **2017**, *56*, 1720−1739.

(3) Li, W. C.; Tse, H. F.; Fok, L. Plastic Waste in the Marine Environment: A Review of Sources, Occurrence and Effects. *Sci. Total Environ.* **2016**, *566-567*, 333−349.

(4) Ter Halle, A.; Jeanneau, L.; Martignac, M.; Jardé, E.; Pedrono, B.; Brach, L.; Gigault, J. Nanoplastic in the North Atlantic Subtropical Gyre. *Environ. Sci. Technol.* **2017**, *51*, 13689−13697.

(5) Mintenig, S. M.; Bäuerlein, P. S.; Koelmans, A. A.; Dekker, S. C.; van Wezel, A. P. Closing the Gap between Small and Smaller: Towards a Framework to Analyse Nano- and Microplastics in Aqueous Environmental Samples. *Environ. Sci.: Nano* **2018**, *5*, 1640−1649.

(6) Schwaferts, C.; Niessner, R.; Elsner, M.; Ivleva, N. P. Methods for the Analysis of Submicrometer- and Nanoplastic Particles in the Environment. *TrAC, Trends Anal. Chem.* **2019**, *112*, 52−65.

(7) Jordan, A.; Haidacher, S.; Hanel, G.; Hartungen, E.; Märk, L.; Seehauser, H.; Schottkowsky, R.; Sulzer, P.; Märk, T. D. A High Resolution and High Sensitivity Proton-Transfer-Reaction Time-of-Flight Mass Spectrometer (PTR-TOF-MS). *Int. J. Mass Spectrom.* **2009**, *286*, 122−128.

(8) Holzinger, R.; Williams, J.; Herrmann, F.; Lelieveld, J.; Donahue, N. M.; Röckmann, T. Aerosol Analysis Using a Thermal-Desorption Proton-Transfer-Reaction Mass Spectrometer (TD-PTR-MS): A New Approach to Study Processing of Organic Aerosols. *Atmos. Chem. Phys.* **2010**, *10*, 2257−2267.

(9) Materić, D.; Peacock, M.; Kent, M.; Cook, S.; Gauci, V.; Röckmann, T.; Holzinger, R. Characterisation of the Semi-Volatile Component of Dissolved Organic Matter by Thermal Desorption − Proton Transfer Reaction − Mass Spectrometry. *Sci. Rep.* **2017**, *7*, 15936.

(10) Materić, D.; Ludewig, E.; Xu, K.; Röckmann, T.; Holzinger, R. Brief Communication: Analysis of Organic Matter in Surface Snow by PTR-MS − Implications for Dry Deposition Dynamics in the Alps. *Cryosphere* **2019**, *13*, 297−307.

(11) Peacock, M.; Materić, D.; Kothawala, D. N.; Holzinger, R.; Futter, M. N. Understanding Dissolved Organic Matter Reactivity and Composition in Lakes and Streams Using Proton-Transfer-Reaction Mass Spectrometry (PTR-MS). *Environ. Sci. Technol. Lett.* **2018**, *5*, 739−744.

(12) Materić, D. Analysis of Organic Matter in Surface Snow by PTR-MS − Implications for Dry Deposition Dynamics in the Alps. *Utrecht University* **2019**, DOI: 10.24416/UU01-6LY8GT.

(13) Holzinger, R. PTRwid: A New Widget Tool for Processing PTR-TOF-MS Data. *Atmos. Meas. Tech.* **2015**, *8*, 3903−3922.

(14) Cappellin, L.; Karl, T.; Probst, M.; Ismailova, O.; Winkler, P. M.; Soukoulis, C.; Aprea, E.; Märk, T. D.; Gasperi, F.; Biasioli, F. On Quantitative Determination of Volatile Organic Compound Concentrations Using Proton Transfer Reaction Time-of-Flight Mass Spectrometry. *Environ. Sci. Technol.* **2012**, *46*, 2283−2290.

(15) Lindinger, W.; Hansel, A.; Jordan, A. On-Line Monitoring of Volatile Organic Compounds at Pptv Levels by Means of Proton-Transfer-Reaction Mass Spectrometry (PTR-MS) Medical Applications, Food Control and Environmental Research. *Int. J. Mass Spectrom. Ion Processes* **1998**, *173*, 191−241.

(16) Holzinger, R.; Acton, W. J. F.; Bloss, W. J.; Breitenlechner, M.; Crilley, L. R.; Dusanter, S.; Gonin, M.; Gros, V.; Keutsch, F. N.; Kiendler-Scharr, A.; Kramer, L. J.; Krechmer, J. E.; Languille, B.; Locoge, N.; Lopez-Hilfiker, F.; Materić, D.; Moreno, S.; Nemitz, E.; Quéléver, L. L. J.; Sarda Esteve, R.; Sauvage, S.; Schallhart, S.; Sommariva, R.; Tillmann, R.; Wedel, S.; Worton, D. R.; Xu, K.; Zaytsev, A. Validity and Limitations of Simple Reaction Kinetics to Calculate Concentrations of Organic Compounds from Ion Counts in PTR-MS. *Atmos. Meas. Tech.* **2019**, *12*, 6193−6208.

(17) Salvador, C. M.; Ho, T.-T.; Chou, C. C.-K.; Chen, M.-J.; Huang, W.-R.; Huang, S.-H. Characterization of the Organic Matter in Submicron Urban Aerosols Using a Thermo-Desorption Proton-Transfer-Reaction Time-of-Flight Mass Spectrometer (TD-PTR-TOF-MS). *Atmos. Environ.* **2016**, *140*, 565−575.

(18) Duemichen, E.; Eisentraut, P.; Celina, M.; Braun, U. Automated Thermal Extraction-Desorption Gas Chromatography Mass Spectrometry: A Multifunctional Tool for Comprehensive Characterization of Polymers and Their Degradation Products. *J. Chromatogr. A* **2019**, *1592*, 133−142.

(19) Cai, L.; Wang, J.; Peng, J.; Tan, Z.; Zhan, Z.; Tan, X.; Chen, Q. Characteristic of Microplastics in the Atmospheric Fallout from Dongguan City, China: Preliminary Research and First Evidence. *Environ. Sci. Pollut. Res.* **2017**, *24*, 24928−24935.

(20) Dris, R.; Gasperi, J.; Saad, M.; Mirande, C.; Tassin, B. Synthetic Fibers in Atmospheric Fallout: A Source of Microplastics in the Environment? *Mar. Pollut. Bull.* **2016**, *104*, 290−293.

(21) Allen, S.; Allen, D.; Phoenix, V. R.; Roux, G. L.; Jiménez, P. D.; Simonneau, A.; Binet, S.; Galop, D. Atmospheric Transport and Deposition of Microplastics in a Remote Mountain Catchment. *Nat. Geosci.* **2019**, *12*, 339.

(22) Tian, L.; Chen, Q.; Jiang, W.; Wang, L.; Xie, H.; Kalogerakis, N.; Ma, Y.; Ji, R. A Carbon-14 Radiotracer-Based Study on the Phototransformation of Polystyrene Nanoplastics in Water versus in Air. *Environ. Sci.: Nano* **2019**, *6*, 2907−2917.

(23) Greilinger, M.; Schöner, W.; Winiwarter, W.; Kasper-Giebl, A. Temporal Changes of Inorganic Ion Deposition in the Seasonal Snow Cover for the Austrian Alps (1983−2014). *Atmos. Environ* **2016**, *132*, 141−152.

(24) Kasper, A.; Puxbaum, H. Seasonal Variation of SO_2, HNO_3, NH_3 and Selected Aerosol Components at Sonnblick (3106ma.s.l.). *Atmos. Environ.* **1998**, *32*, 3925−3939.

(25) Kasper-Giebl, A.; Kalina, M. F.; Puxbaum, H. Scavenging Ratios for Sulfate, Ammonium and Nitrate Determined at Mt. Sonnblick (3106m a.s.l.). *Atmos. Environ.* **1999**, *33*, 895−906.